MOLECULAR AND CELLULAR BIOLOGY, Oct. 2008, p. 6314–6328 Vol. 28, No. 20
0270-7306/08/$08.00+0 doi:10.1128/MCB.00763-08

Tissue-Specific Role of Glycogen Synthase Kinase 3β in Glucose Homeostasis and Insulin Action▽†

Satish Patel,[1] Bradley W. Doble,[1,2] Katrina MacAulay,[1] Elaine M. Sinclair,[1] Daniel J. Drucker,[1] and James R. Woodgett[1]*

Samuel Lunenfeld Research Institute, Mount Sinai Hospital, 600 University Avenue, Toronto, Ontario M5G 1X5, Canada,[1] *and McMaster Stem Cell and Cancer Research Institute, McMaster University, 1200 Main Street West, Hamilton, Ontario L8N 3Z5, Canada*[2]

Received 12 May 2008/Returned for modification 7 July 2008/Accepted 31 July 2008

Dysregulation of the protein kinase glycogen synthase kinase 3 (GSK-3) has been implicated in the development of type 2 diabetes mellitus. GSK-3 protein expression and kinase activity are elevated in diabetes, while selective GSK-3 inhibitors have shown promise as modulators of glucose metabolism and insulin sensitivity. There are two GSK-3 isoforms in mammals, GSK-3α and GSK-3β. Mice engineered to lack GSK-3β die in late embryogenesis from liver apoptosis, whereas mice engineered to lack GSK-3α are viable and exhibit improved insulin sensitivity and hepatic glucose homeostasis. To assess the potential role of GSK-3β in insulin function, a conditional gene-targeting approach whereby mice in which expression of GSK-3β was specifically ablated within insulin-sensitive tissues were generated was undertaken. Liver-specific GSK-3β knockout mice are viable and glucose and insulin tolerant and display "normal" metabolic characteristics and insulin signaling. Mice lacking expression of GSK-3β in skeletal muscle are also viable but, in contrast to the liver-deleted animals, display improved glucose tolerance that is coupled with enhanced insulin-stimulated glycogen synthase regulation and glycogen deposition. These data indicate that there are not only distinct roles for GSK-3α and GSK-3β within the adult but also tissue-specific phenotypes associated with each of these isoforms.

Glycogen synthase kinase 3 (GSK-3) is a highly conserved, ubiquitously expressed serine/threonine protein kinase that exists as two isoforms, GSK-3α (51 kDa) and GSK-3β (47 kDa), which are encoded by separate genes that produce highly homologous proteins that differ significantly only in their N- and C-terminal regions (50). GSK-3 is highly active under resting conditions and is rapidly inactivated by insulin through phosphorylation of an N-terminal domain serine residue (Ser 21 of GSK-3α and Ser 9 of GSK-3β) (43). Insulin inhibition of GSK-3 requires the activation of phosphatidylinositol 3-kinase and protein kinase B (PKB/Akt), with PKB/Akt phosphorylating both isoforms of GSK-3 on these regulatory serine residues (11). GSK-3 was originally identified as a regulator of glycogen synthase (GS), a rate-limiting enzyme that promotes glycogen deposition (17). In the absence of insulin, active GSK-3 phosphorylates four serine residues in the C-terminal domain of GS and negatively regulates its activity, reducing the capacity of cells to synthesize and store glycogen (25). Inhibition of GSK-3 by insulin (via Ser 9/21 phosphorylation) results in the dephosphorylation and activation of GS, leading to increased rates of glycogen synthesis (15, 35).

A major feature of type 2 diabetes mellitus (T2DM) is impairment of both basal and insulin-stimulated glucose metabolism in insulin-responsive, peripheral tissues, including skeletal muscle (SM) and liver (2, 37, 41). While there are no known disease-associated mutations in the two GSK-3 genes (21), there are data that show elevation of GSK-3 expression and activity in the SM of patients with T2DM and in adipose tissues of obese diabetic mice (16, 33). Furthermore, transgenic overexpression of GSK-3β in the SM of mice results in impaired glucose tolerance, elevated plasma insulin levels, and reduced glycogen content (36). Conversely, GSK-3 inhibitors can mimic insulin action in cell lines and tissues (8, 27, 29, 34), while administration of GSK-3 inhibitors to rodent models of obesity and T2DM improves insulin sensitivity and glucose homeostasis by increasing glycogen synthesis and coordinately reducing glucose output by inhibiting hepatic gluconeogenesis (9, 14, 20, 24; reviewed in reference 40).

Given that chemical inhibitors of GSK-3 are unable to discriminate between the two isoforms, it is not possible to evaluate isoform-specific functions of GSK-3α and GSK-3β by using these drugs. However, evidence for isoform-specific roles has emerged from mouse models. Mice engineered to lack GSK-3β (but still retaining GSK-3α) die during embryogenesis (23). Interestingly, mice that lack GSK-3α (retaining GSK-3β) are viable and display improved whole-body glucose tolerance and hepatic insulin sensitivity (28). Furthermore, insulin regulation of GS is completely abolished in the SM of homozygous "knock-in" mice expressing an insulin-insensitive mutant (S9A) of GSK-3β, whereas in GSK-3α (S21A) knock-in mice, GS activity is unaltered (30). These findings suggest that there are GSK-3α and GSK-3β tissue- and isoform-specific roles in regulation of glucose metabolism.

Due to the embryonic lethality of global GSK-3β knockout (KO) mice, we employed a conditional gene-targeting approach to derive mice that selectively lack GSK-3β expression in two major insulin-sensitive tissues. Here, we report that

* Corresponding author. Mailing address: Samuel Lunenfeld Research Institute, Mount Sinai Hospital, 600 University Avenue, Toronto, Ontario M5G 1X5, Canada. Phone: (416) 586-8811. Fax: (416) 586-8839. E-mail: woodgett@mshri.on.ca.

† Supplemental material for this article may be found at http://mcb.asm.org/.

▽ Published ahead of print on 11 August 2008.

liver-specific and SM-specific GSK-3β KO mice display different phenotypes with respect to glucose metabolism. While the *l*iver-specific GSK-3β *KO* (LβKO) mice exhibited normal metabolic characteristics, S*M*-specific GSK-3β *KO* (MβKO) mice displayed improved glucose tolerance and more-effective GS activation. The GSK-3β tissue-specific KO mice provide new genetic tools for the analysis of isoform- and tissue-specific roles of GSK-3 in cellular regulation and enable the therapeutic potential of GSK-3 inhibitors in the treatment of T2DM to be more thoroughly assessed.

MATERIALS AND METHODS

Construction of the GSK-3β-targeting vector. The genomic region flanking exon 2 of the GSK-3β gene was isolated from a lambda phage clone library containing genomic DNA from the mouse strain 129/Ola. The "arms" of homology for the targeting vector were obtained by PCR amplification of the GSK-3β genomic regions by use of Platinum Pfx (Invitrogen) and inserted into the backbone targeting vector pSPUC. LoxP sites were introduced by PCR into the intronic region flanking exon 2 of the GSK-3β gene, while the neomycin resistance cassette was inserted and flanked by FLP recombination target (FRT) sites. The fragments were sequenced for any PCR-generated errors.

Generation of GSK-3β-floxed targeted mice and tissue-specific KO mice. The R1 mouse embryonic stem (ES) cell line was obtained from Andras Nagy (Samuel Lunenfeld Research Institute [SLRI]) and maintained in "KO" Dulbecco's modified Eagle's medium containing a high concentration of glucose supplemented with 15% fetal bovine serum (HyClone), 0.1 mM nonessential amino acids, antibiotics (100 units penicillin G, 100 μg/ml streptomycin), 2 mM L-glutamine, 1 mM sodium pyruvate, 0.1 mM 2-mercaptoethanol, and 1,000 units/ml ESGRO (Chemicon).

Thirty micrograms of the GSK-3β-targeting vector was linearized and electroporated into R1 ES cells (6×10^6 cells/ml) by using a Bio-Rad Gene Pulser II instrument (250 V, 500 μF), and the cells were then plated onto gelatinized plates in the presence of 250 μg/ml of G418. One hundred twenty G418-resistant colonies were screened by PCR, and 15 ES cell clones that had undergone correct homologous recombination were identified. Two ES cell clones with optimal morphologies were microinjected into C57/B6J blastocysts, which were then reimplanted into recipient female mice. Chimeric mice that had high degrees of ES cell contribution were identified by coat color and were then crossed with C57/B6J, and germ line transmission of the GSK-3β-floxed allele was verified by PCR (with only one of the ES cell lines achieving germ line transmission). These GSK-3β-floxed mice were subsequently crossed with B6 mice that carried the FLPe recombinase (JAX Lab) to remove the *neo* cassette that resides within the intronic region of the GSK-3β-targeting vector. Resultant interbreeding of these mice yielded GSK-3β-floxed (FL/FLβ) mice that were viable, healthy, and born at the expected Mendelian frequency.

To generate liver-specific GSK-3β KO animals, the GSK-3β-floxed mice were crossed with the B6.Cg-Tg(Alb-Cre)21Mgn/J (Jackson Laboratory) strain, which carries Cre recombinase under the control of the albumin promoter. These GSK-3β Fl/FL AlbCre$^+$ mice (B6/129 background, F3 backcross) are designated LβKO, denoting them as *l*iver-specific GSK-3β *KO*.

With a similar breeding strategy, SM-specific GSK-3β KO animals were generated by breeding the conditionally targeted GSK-3β KO mice with mice expressing Cre under the control of the myosin light chain 1*f* (MLC1*f*) promoter (kindly provided by Steve Burden, Skirball Institute, NY) (5). These GSK-3β Fl/FL MLC1*f*-cre$^+$ mice (B6/129/ICR background, F3 backcross) are denoted MβKO, indicating an S*M*-specific GSK-3β *KO*. Genotypes for the various tissue-specific deletions were confirmed by PCR for the presence of Cre and for the detection of the deleted, floxed GSK-3β allele.

The GSK-3β FL/FL lines demonstrated expression levels of GSK-3 protein as well as other components of the insulin-signaling pathway similar to those for wild-type (WT) animals (data not shown). We performed additional experiments to demonstrate that the presence of the Alb-cre or MLC-cre transgene in WT animals with respect to GSK-3 had no significant effects on the metabolic profiles (as assessed by glucose tolerance tests [GTT] and insulin tolerance tests [ITT]) analyzed in these studies (data not shown). In addition, all studies were performed with respective littermate controls to control for possible environmental influences. GSK-3β FL/FL control mice and the tissue-specific KO mice were housed five per cage under a light/dark cycle of 12 h each in the Ontario Cancer Institute animal facility, with free access to food and water except where noted. All procedures were conducted according to protocols and guidelines approved by the Ontario Cancer Institute Animal Care Committee.

GTT and ITT. Following an overnight fast (16 to 18 h for the GTT) or a 5-h fast (for the ITT), mice were injected intraperitoneally (i.p.) with 1 mg/g of glucose (for the GTT) or 0.75 mU/g insulin (for the ITT), and blood glucose (tail vein blood) was measured using a OneTouch UltraSmart blood glucose monitoring system (Lifescan, Canada) at the indicated times. For certain studies involving fasted and fed animals, measurements were taken between 8:00 and 10:00 a.m. for both fasted (overnight, 16 to 18 h) and fed (ad libitum) cohorts.

Determination of plasma insulin, adiponectin, and triglycerides. Blood samples were collected from the tail veins of mice fasted overnight (16 to 18 h) and either treated or not treated with 1 mg/g glucose (i.p) for 15 min and centrifuged at 6,000 × *g* for 10 min, and the plasma supernatant was collected. The plasma insulin and adiponectin levels were measured using a Mercodia ultrasensitive insulin enzyme-linked immunosorbent assay kit (Alpco Diagnostics) and an adiponectin enzyme-linked immunosorbent assay kit (Linco Research), respectively. Plasma triglycerides were determined using a Wako L-type triglyceride H kit (Wako Chemicals, USA, Inc.).

In vivo SM glucose uptake. After an overnight fast, mice were injected i.p. with 2-deoxy-D-[1,2-^{3}H]glucose mixed with 20% dextrose (2 g/kg body weight; 10 μCi/mouse), and the accumulation of radiolabeled 2-deoxy-D-glucose in SM was measured as described previously (53).

Glucose transport assay with isolated muscle. After an overnight fast, animals were deeply anesthetized using Avertin, intact whole-extensor digitorum longus (EDL) and soleus muscles were isolated and incubated in the absence or presence of 2 mU/ml insulin, and the uptake of 2-deoxyglucose (2DG) was measured as described previously (49).

Determination of glycogen content. Fifty milligrams of gastrocnemius muscle or 20 mg liver tissue was acid hydrolyzed in 2 N HCl by heating it at 95°C for 2 h and neutralized using 2 N NaOH. The liberated free-glycosyl units were assayed spectrophotometrically by using a glucose reagent hexokinase-dependent-assay kit (Amresco, OH) as previously described (4). Glycogen was also visualized in paraffin-embedded tissue sections by using a periodic acid-Schiff (PAS) staining kit (Sigma Aldrich). Tissue sections were also stained with standard hematoxylin and eosin for general cell morphology.

Isolation of primary hepatocytes. Eight- to 12-week old LβKO and GSK-3β FL/FL littermate control animals were anesthetized and primary hepatocytes isolated by a retrograde, nonrecirculating in situ liver perfusion with collagenase as described previously (28).

Tissue lysate preparation. Following an overnight fast, mice were either treated with 100 mU/g insulin, 1 mg/g glucose or refed (by placing standard chow pellets back into cages) for various times. After cervical dislocation, mouse tissues were dissected and quickly frozen in liquid N_2 and stored for subsequent processing or were lysed immediately. Fresh or snap-frozen tissues were lysed in 50 mM NaCl, 25 mM PIPES [piperazine-*N*,*N*′-bis(2-ethanesulfonic acid)], pH 7, 0.5% NP-40, 5 mM EGTA, 25 mM NaF, 1 mM Na-orthovanadate, 10 mM Na–β-glycerophosphate, 1 mM sodium pyrophosphate, phosphatase inhibitor cocktail (Sigma), and a protease inhibitor cocktail tablet (Roche) by using a 2-ml Kontes tissue grinder. Tissue homogenates were cleared by centrifugation at 16,000 × *g* for 15 min at 4°C, and protein concentration was determined by a Bio-Rad DC protein assay. The supernatants were stored at −80°C until analysis.

Immunoblotting. Twenty micrograms of protein lysates was denatured in sodium dodecyl sulfate (SDS) sample buffer and resolved by SDS-polyacrylamide gel electrophoresis, and proteins were transferred onto polyvinylidene difluoride membranes. Membranes were blocked with 5% nonfat dry milk for 1 h at room temperature and incubated with antibodies directed against the following antigens: phospho-GS Ser 641, phospho-GSK-3α/β Ser9/Ser21, phospho-PKB/Akt Ser 473, and PKB/Akt (Cell Signaling Technologies); muscle GS, GLUT1, and GLUT4 (Chemicon); GSK-3α/β (Biosource) and β-catenin (BD Transduction Laboratories); liver GS (gift from J. Guinovart, University of Barcelona); glycogen phosphorylase and phosphorylase phosphoserine 15 (gift from Tricia Cohen, University of Dundee); and glyceraldehyde-3-phosphate dehydrogenase (GAPDH) or caveolin-1 (Santa Cruz). Following antibody incubation, the membranes were washed five times in Tris-buffered saline-0.1% Tween-20 prior to incubation with horseradish peroxidase (HRP)-conjugated anti-rabbit immunoglobulin G (IgG), HRP-conjugated anti-mouse IgG, or HRP-conjugated anti-sheep IgG secondary antibodies. The bands were visualized using SuperSignal Western Pico chemiluminescence reagent (Pierce) and quantified using an Alpha Innotech FluorChem HD2 documentation system.

GS assays. Frozen SM and liver tissue samples were minced using 1 ml homogenization buffer (50 mM Tris, pH 7.8, 100 mM NaF, 10 mM EDTA, 5% glycerol, and a protease inhibitor cocktail tablet) and homogenized using a Brinkman Polytron. The tissue homogenates were cleared by centrifugation at

3,000 × *g* for 10 min at 4°C, and GS activity from the supernatants was assayed according to the method of Thomas et al. (46) based on incorporation of UDP-[^{3}H]glucose into glycogen. Immunoblot analysis performed under these conditions demonstrated that regulated phosphorylation of GS was maintained (data not shown).

Glycogen phosphorylase assays. Glycogen phosphorylase activity was determined by measuring the incorporation of [^{14}C]glucose-1-phosphate into glycogen in the absence or presence of 2 mM AMP as previously described (7).

GSK-3 kinase assays. Assays of GSK-3 were performed on mouse tissue extracts as described previously (13), with the following modifications. Briefly, 0.1 g of muscle or liver tissue was lysed in 3 ml of detergent-free lysis buffer (50 mM Tris-HCl, 4 mM EDTA, 2 mM EGTA, 10 mM Na–β-glycerophosphate, 5 mM NaF, 1 mM phenylmethylsulfonyl fluoride, 1 mM Na-orthovanadate, and protease and phosphatase inhibitor cocktails, pH 7) and homogenized using a 2 ml Kontes tissue grinder. The tissue homogenate was centrifuged at 4,000 × *g* for 30 min at 4°C and the supernatant applied to a chilled, carboxymethyl (CM)-Sepharose fast-flow resin column (Amersham) preequilibrated with 25 mM Tris-HCl, 2 mM EDTA, 1 mM EGTA, 10 mM Na–β-glycerophosphate, 2.5% glycerol, 5 mM NaF, 1 mM phenylmethylsulfonyl fluoride, 1 mM orthovanadate, and protease and phosphatase inhibitor cocktails, pH 7 (buffer A). The column was washed with 5 column volumes of low-salt wash buffer (buffer A plus 20 mM NaCl) and GSK-3 eluted using buffer A plus 250 mM NaCl. Fractions containing the highest concentrations of protein were pooled and used in a kinase assay to assess GSK-3 activity as described in reference 13.

Extraction of total muscle membrane. Muscle tissue (0.1 g) was minced using 0.5 ml homogenization buffer (20 mM $NaHCO_3$, 250 mM sucrose, 5 mM NaN_3, 1 mM EDTA, and a protease inhibitor cocktail tablet), homogenized using a Brinkman Polytron, and clarified by centrifugation at 1,300 × *g* for 10 min. The supernatant was saved, and the pellet was resuspended in 0.5 ml of homogenization buffer, rehomogenized, and centrifuged. The resulting supernatant was pooled with the first supernatant and recentrifuged at 9,000 × *g* for 10 min at 4°C. The resultant pellet was resuspended in 0.5 ml homogenization buffer and centrifuged at 229,000 × *g* for 90 min at 4°C, and the total membrane pellet was resuspended in 0.3 ml homogenization buffer and the protein concentration determined.

Statistical analysis. For multiple comparisons, statistical analysis was performed using either two-way analysis of variance followed by a Bonferroni posttest or unpaired Student *t* tests. Data analysis was performed using GraphPad Prism or Microsoft Excel.

RESULTS

Generation of mice harboring conditional alleles of GSK-3β. Mice expressing a conditional allele of GSK-3β were generated as described in Materials and Methods (Fig. 1). GSK-3β FL/FL (FL/FLβ) or GSK-3β$^+$/FL (data not shown) mice expressed GSK-3β levels equivalent to those in WT animals (GSK-3β$^{+/+}$ or GSK-3β$^{+/+}$ AlbCre$^+$) as judged by immunoblotting (Fig. 2C), indicating that the LoxP sites flanking exon 2 did not interfere with expression of the gene (Fig. 2D).

Liver-specific GSK-3β KO mice are viable and develop normally. The liver plays a central role in glucose homeostasis, responsible for regulating postprandial glucose uptake and production/output (6). To generate mice lacking GSK-3β within the liver, GSK-3β-floxed mice were crossed with a transgenic strain expressing Cre under the control of the hepatocyte-specific albumin promoter. The resultant tissue-specific (GSK-3β FL/FL Alb Cre) KO mice, termed *l*iver-specific GSK-3β *KO* (LβKO), were viable, fertile, and born at the expected Mendelian frequency and displayed whole-body (Fig. 2A) and liver (data not shown) weights similar to those of their GSK-3β FL/FL (FL/FLβ) littermates. PCR (Fig. 2B) and immunoblot (Fig. 2C) analyses demonstrated that the deletion of the GSK-3β-floxed allele with consequent loss (>90%) of protein expression occurred specifically within the liver and not in other tissues of the KO animal (Fig. 2D). The residual expression in the KO tissue most likely reflects GSK-3β protein expression in nonhepatic cells (e.g., endothelial cells or Kupffer cells), which account for approximately 10% of the cell population within the liver and do not express *alb*-Cre (39).

Liver-specific GSK-3β KO mice display normal metabolic characteristics. Mice treated with GSK-3 inhibitors or engineered to lack GSK-3α display improved hepatic glucose homeostasis and insulin sensitivity (20, 28). We therefore investigated whether loss of liver GSK-3β affected whole-body glucose homeostasis. GTT and ITT performed on LβKO and GSK-3β FL/FL littermates at either 8 weeks or 6 months of age revealed no statistically significant differences in the rate of glucose clearance upon i.p. administration of glucose or insulin (Fig. 3A). Furthermore, no significant differences were found in blood glucose levels between fasted or fed LβKO and GSK-3β FL/FL animals (see Fig. S1 in the supplemental material).

Liver and SM are two well-characterized tissues responsible for the disposal of the majority of a glucose load and for the storage of this glucose as glycogen. We determined the glycogen levels in fasted and fed tissues from LβKO and GSK-3β FL/FL control mice. Upon examination of PAS reagent-stained, paraffin-embedded tissue sections, no significant differences were observed in accumulation of glycogen in liver (Fig. 3B) or SM (data not shown) between the two groups. This finding was independently confirmed by biochemical quantification of glycogen with an acid hydrolysis technique applied to frozen tissue samples (Fig. 3C).

Analysis of insulin signaling in liver-specific GSK-3β KO mice. Insulin modulates the activities of PKB/Akt, GSK-3, and GS by phosphorylation. Phosphorylation of PKB/Akt at Thr 308 and Ser 473 results in its activation, whereas phosphorylation of GSK-3 (Ser 21 of GSK-3α and Ser 9 of GSK-3β) and GS (Ser 641, Ser 645, Ser 649, and Ser 653) inhibits these enzymes. We investigated whether lack of hepatic GSK-3β affected the activation of the insulin-signaling pathway. Levels of insulin-induced activation of PKB/Akt were similar in the livers of both LβKO and GSK-3β FL/FL mice, as judged by quantification of immunoreactivity to the phospho-Ser 473 PKB/Akt antibody (Fig. 4A). Indeed, levels of insulin-induced phosphorylation and activation of other signaling proteins, such as S6 kinase (S6K) and ribosomal S6 protein, were also similar in primary hepatocytes isolated from LβKO and GSK-3β FL/FL mice (Fig. 4B). Furthermore, the levels of expression and insulin-induced phosphorylation of GSK-3α at Ser 21 remained equal for the two groups, indicating that there was no compensatory regulation of the remaining GSK-3α isoform in the LβKO mice (Fig. 4A and B and 2C). GSK-3 assays derived from partially purified liver extracts revealed that total GSK-3 activity was reduced by approximately 50% (55.9% ± 5%) in the LβKO mice compared to that in FL/FLβ control animals (Fig. 4C).

It is well established that in SM and liver tissue, GS is regulated by covalent phosphorylation, which inhibits the enzyme and by the allosteric coactivator glucose-6-phosphate (G6P) (3, 30). Using a phospho-specific antibody directed against one of the four GSK-3-specific sites, Ser 641, we found that administration of glucose (15 min) or 2 h of feeding after fasting induced marked degrees of dephosphorylation of GS that were similar in the livers of the control FL/FLβ and LβKO mice (Fig. 4A). Furthermore, the levels of activation of GS

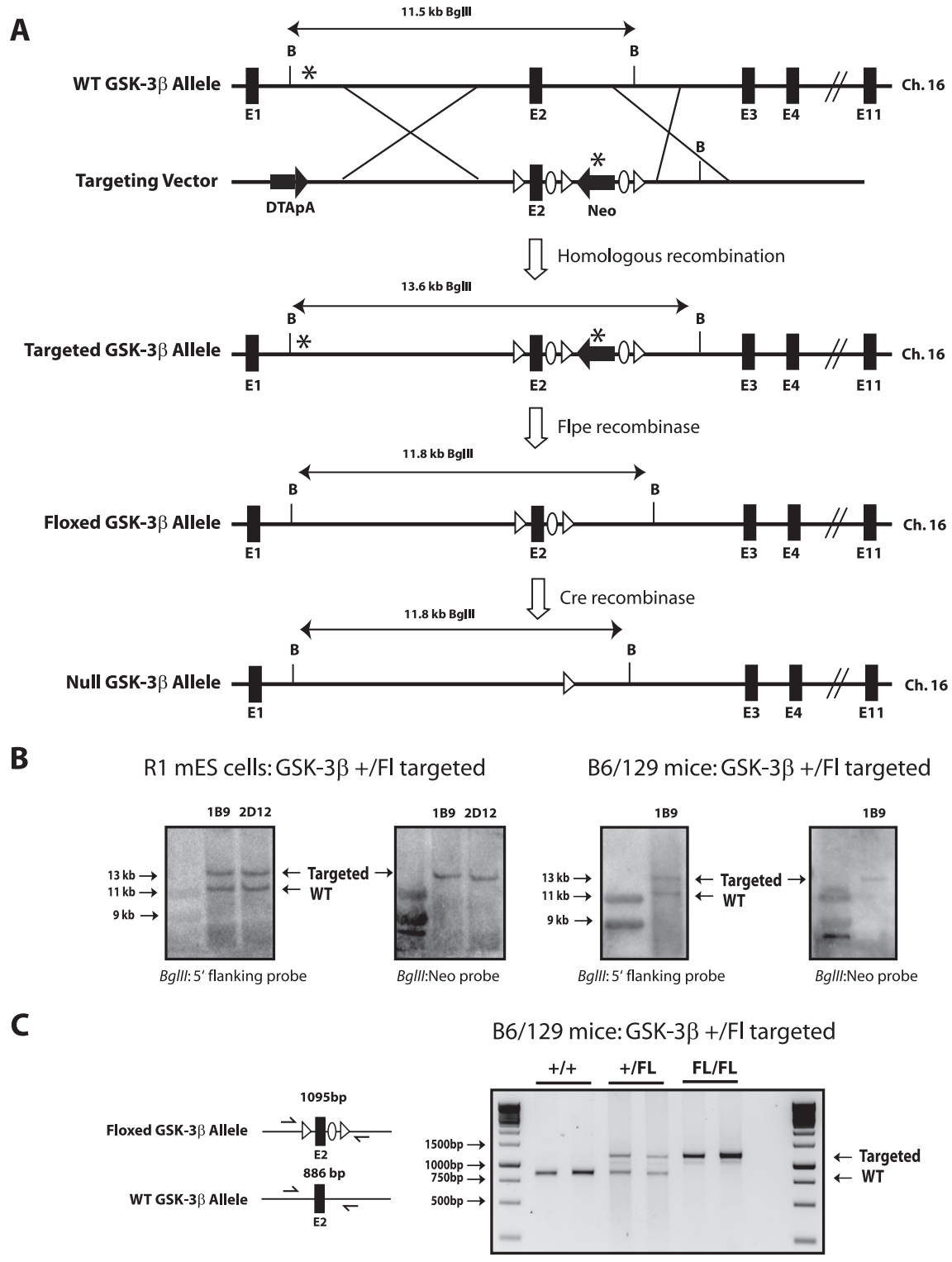

FIG. 1. Generation of conditional GSK-3β-floxed (FL), targeted mice. (A) Schematic outline describing the targeting strategy for generating conditional GSK-3β-floxed (FL) mice and the subsequent tissue-specific KO mice. After homologous recombination with the targeting vector, exon 2 (E2) of the GSK-3β gene was replaced with a LoxP-flanked (floxed) exon 2 and an FRT-flanked neomycin resistance cassette. Mice carrying the GSK-3β-floxed allele were bred to FLPe recombinase-expressing mice to remove the *neo* cassette. Deletion of exon 2, and hence deletion of GSK-3β expression, is achieved by crossing GSK-3β FL mice with strains expressing Cre recombinase under the control of tissue-specific promoters. Triangles, Lox P recombination sites; ovals, FRT recombination sites; B, BglII. Asterisks represent hybridization sites for Southern blot probes. (B) Southern blot analysis. ES cells and mouse tail genomic DNA were digested with BglII and probed with the 5′ GSK-3β or neomycin DNA probe (*), confirming proper targeting of the GSK-3β-floxed allele in R1 mouse ES cell (mES) clones 1B9 and 2D12 and germ line transmission of the GSK-3β-floxed allele (by use of the 1B9 clone) in mice. The 11.8-kb band corresponds to the WT GSK-3β allele, whereas the 13.6-kb band corresponds to the correctly targeted GSK-3β FL allele. (C) PCR genotype analysis of genomic DNA isolated from the progeny of the GSK-3β^{+}/FL F1 cross. The WT GSK-3β band is 886 bp, whereas the GSK-3β FL band is 1,095 bp.

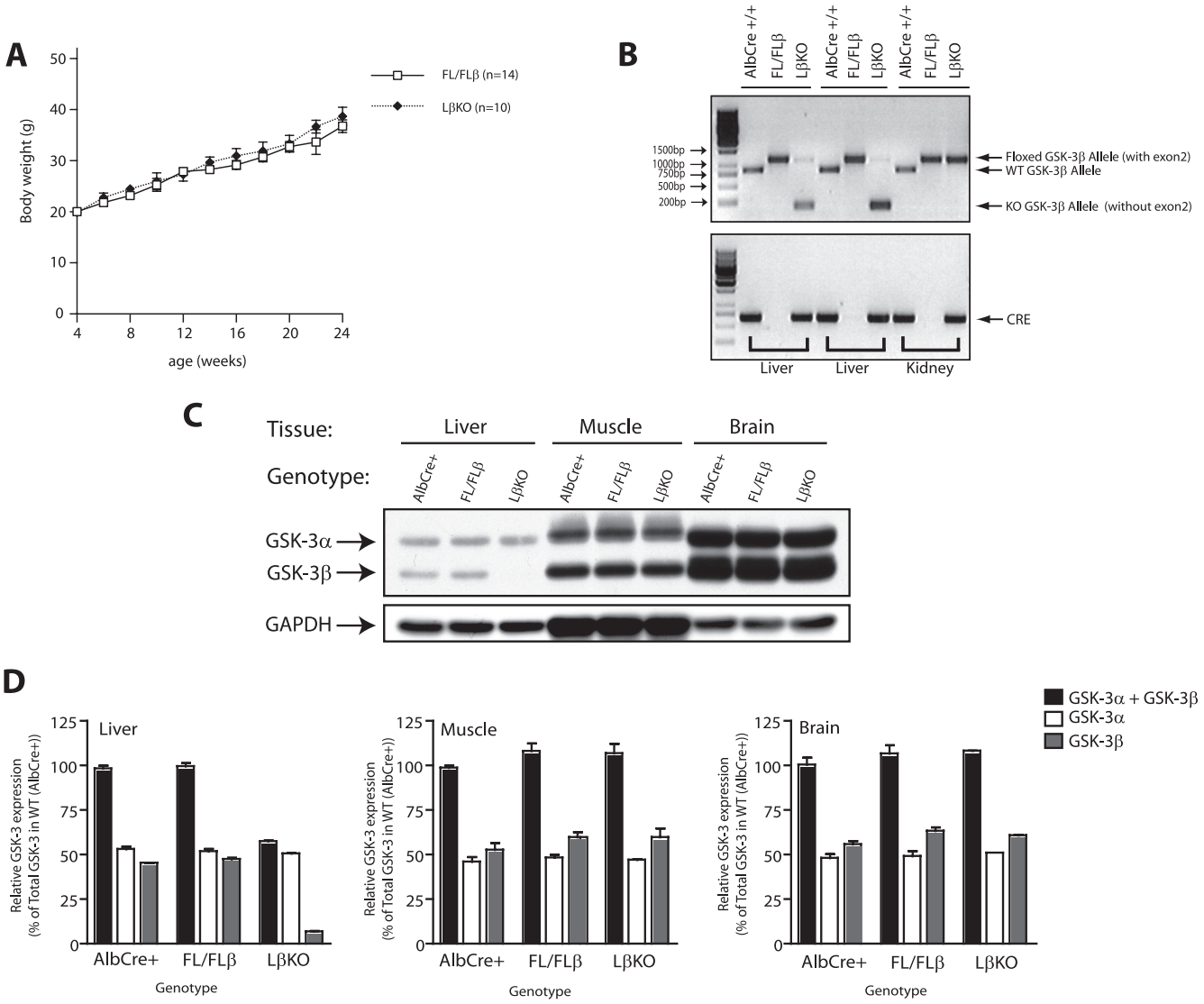

FIG. 2. Generation and characterization of liver-specific GSK-3β KO (LβKO) mice. (A) Weight analysis. Male GSK-3β FL/FL (termed FL/FLβ) control and GSK-3β FL/FL AlbCre$^+$ (termed LβKO) mice were weighed every 2 weeks between the ages of 4 and 24 weeks. Each point represents the mean ± standard error of the mean (SEM), with *n* indicating the number analyzed in each group. No statistical difference in the mean weights was observed between the groups by Student's *t* test. (B) PCR analysis. Genomic DNA was isolated from the tissues stated and analyzed by PCR for Cre-mediated excision of GSK-3β. PCR for GSK-3β (top) demonstrates that exon 2 of the GSK-3β FL allele is excised only in the livers of the LβKO mice, not in those of the control FL/FLβ or the WT AlbCre$^{+/+}$ (littermate control) mice. The bottom panel displays genomic detection of the Cre transgene. (C) Western blot analysis. Tissue extracts from liver, muscle (quadricep) and brain were prepared from 8-week-old male mice of the genotypes indicated and immunoblotted with an antibody that specifically recognizes GSK-3α and GSK-3β. Equal loading of the lanes was assessed using an anti-GAPDH antibody, and the blots shown are representative of three independent experiments. (D) Quantification of GSK-3. The densitometries of GSK-3α and GSK-3β were measured and normalized to GAPDH levels, and the expression of each isoform is displayed relative to the total (GSK-3α plus GSK-3β) expression level in the respective WT (or AlbCre$^+$) tissue.

were similar for the two groups when liver extracts were assayed in the presence of low (0.1 mM) or high (10 mM) concentrations of G6P (Fig. 4D). Analysis of insulin signaling in SM extracts from the control FL/FLβ and LβKO mice revealed no significant differences in insulin-mediated regulation of PKB/Akt, GSK-3, or GS (Fig. 4E).

Deletion of GSK-3β in SM. Glucose uptake into SM accounts for the disposal of 70 to 90% of a glucose load. To evaluate the role of GSK-3β in regulation of glucose homeostasis in SM, we generated S*M*-specific GSK-3β *KO* (MβKO) mice by crossing the GSK-3β-floxed (FL), targeted mice with transgenic animals that expressed Cre-recombinase under the control of the SM-specific *mlc1f* promoter. Like the liver KO animals, MβKO mice were viable, fertile, born at the expected Mendelian frequency, and similar in weight to their FL/FLβ control littermates (Fig. 5A). PCR (Fig. 5B) and immunoblot (Fig. 5C) analyses demonstrated selective and efficient deletion (>90%) of GSK-3β only in SM tissue types, not in cardiac muscle or nonmuscle tissues, demonstrating the tissue specificity of the *mlc1f* gene. As previously reported, the

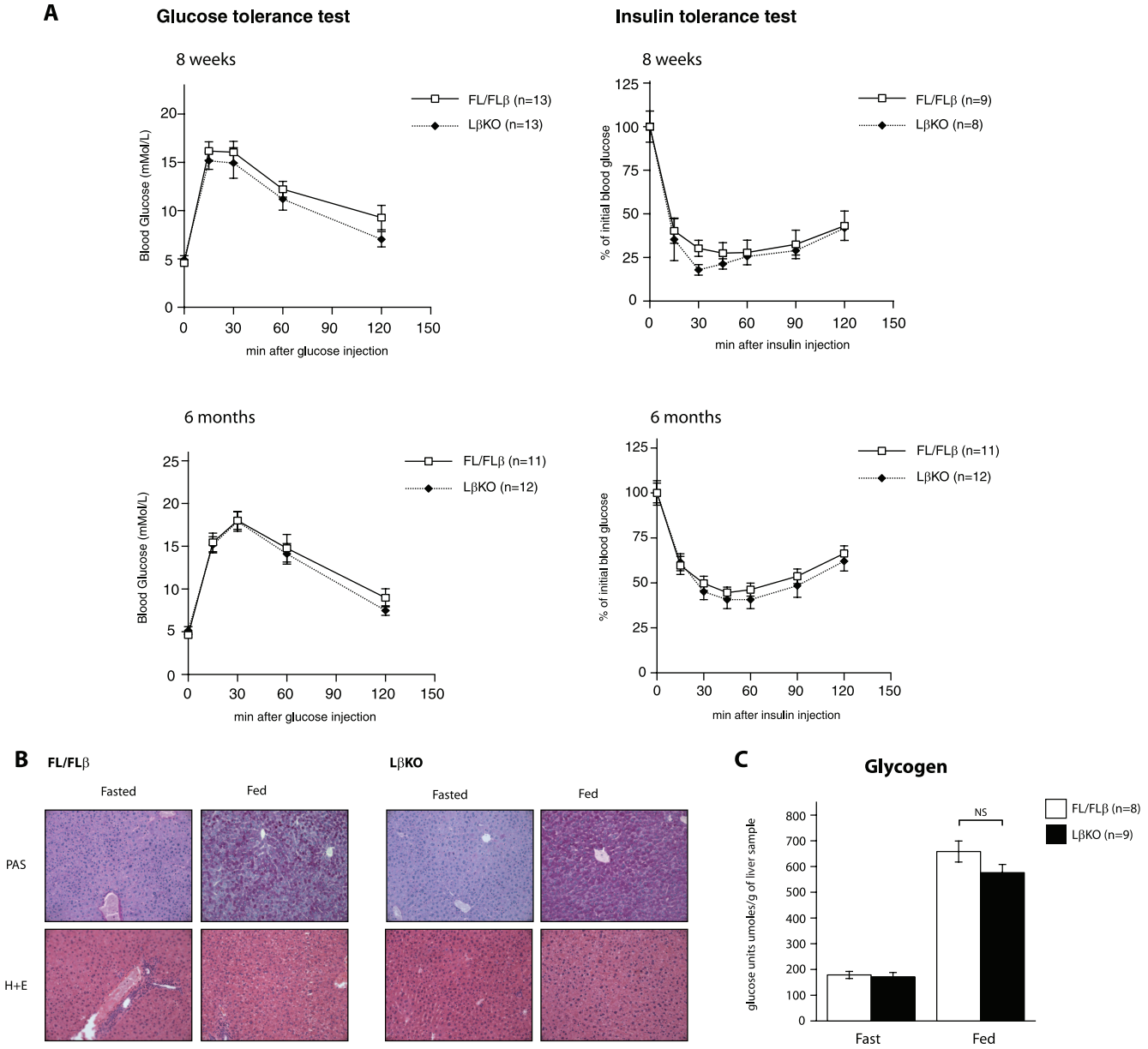

FIG. 3. LβKO mice display "normal" glucose homeostasis and insulin sensitivity. (A) Glucose metabolism profile. GTT and ITT were performed on 8-week- or 6-month-old male FL/FLβ control and LβKO mice as described in Materials and Methods. Values are the means ± SEMs, with *n* indicating the number of mice in each group. (B) Glycogen staining. Liver sections from fasted (overnight, 16 h) or fed (ad libitum) 8-week-old male FL/FLβ control and LβKO mice were stained with PAS to detect glycogen accumulation (dark purple staining; top) or hematoxylin and eosin (H+E) for general cell morphology (bottom). The images are representative of results from five animals. (C) Glycogen content in liver. Liver tissues were extracted from fasted (overnight, 16 h) or fed (ad libitum) 8-week-old male FL/FLβ control and LβKO mice, and glycogen content was determined by acid hydrolysis and is expressed as μmol of glucose units per gram of liver tissue. Data are presented as means ± SEMs, with each liver sample assayed in triplicate, and *n* indicates the number of mice in each group. NS, not significant.

use of the *mlc1f* locus restricts Cre expression to fast/glycolytic fibers, which, in mice, are the overwhelming muscle type, with the exception of the soleus, which is primarily composed of slow/oxidative fibers (5).

SM-specific GSK-3β KO mice exhibit improved glucose homeostasis and enhanced insulin sensitivity. We examined whether selective loss of GSK-3β from SM affected glucose metabolism. Initially, we found no significant differences in blood glucose levels between fasted or fed MβKO and GSK-3β FL/FL animals at 6 to 12 weeks of age (Fig. 6A). However, upon i.p. injection of glucose, MβKO (but not heterozygous GSK-3β^{+}/Fl MLC*f* Cre^{+}) mice (see Fig. S2 in the supplemental material) exhibited a significantly enhanced ability to clear circulating blood glucose, demonstrating improved glucose sensitivity compared to that of their GSK-3β FL/FL counterparts (Fig. 6B). The enhanced glucose tolerance in the MβKO mice was not accompanied by any changes in glucose-stimulated insulin release (Fig. 6B, inset); however, we observed an

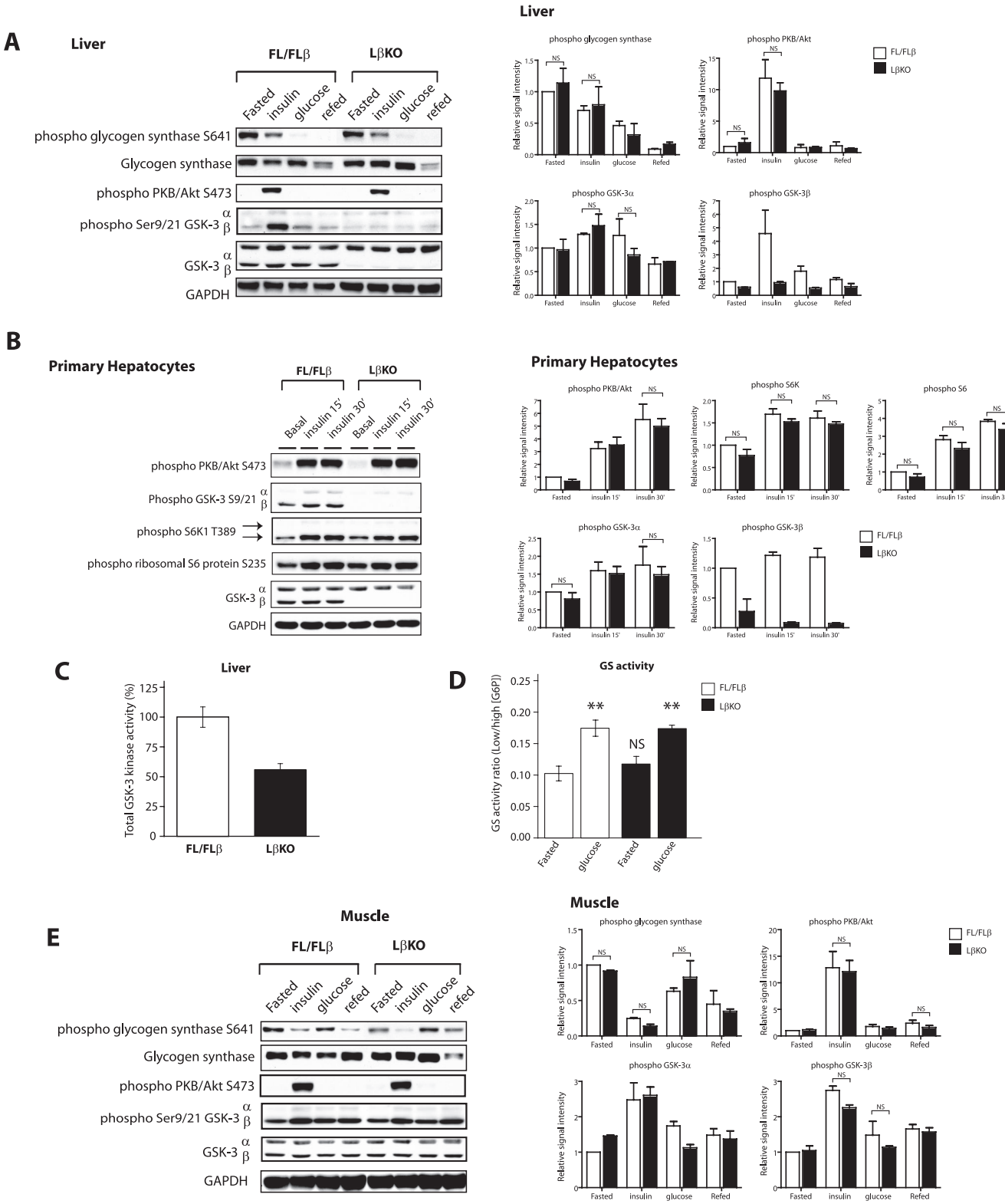

FIG. 4. Analysis of insulin signaling in LβKO mice. (A and E) Insulin signaling in liver (A) and muscle (quadricep) (E) samples. Eight-week-old male FL/FLβ control and LβKO mice were fasted overnight and injected i.p. with 100 mU/g insulin for 15 min or with 1 mg/g glucose for 20 min or were allowed to refeed ad libitum for 2 h. Following treatment, liver (A) and SM (E) tissues were extracted, lysed as described in Materials and Methods, and immunoblotted with the indicated antibodies. Equal loading of the lanes was assessed using an anti-GAPDH antibody, and a representative blot is shown (left) with the quantification of results from four independent experiments displayed (right). Data are presented as a bar graph showing signal intensities compared to that for fasted FL/FLβ mice, which is set as 1. NS, not significant. (B) Insulin signaling in hepatocytes. Primary hepatocytes were isolated from 10-week-old male FL/FLβ control and LβKO mice and serum starved overnight prior to

enhanced ability in the MβKO mice to clear blood glucose upon i.p. administration of insulin (Fig. 6B), which was more pronounced in younger MβKO mice (6 weeks), an effect observed by others (e.g., reference 12).

We also observed improved insulin signaling in SM extracts from MβKO mice. More specifically, insulin-induced dephosphorylation and activation of GS were significantly increased in MβKO mice compared to those in the FL/FLβ controls (Fig. 7A [quantified in panel B, left]). The enhanced GS regulation was in line with the measured enzymatic activity of GS from muscle extracts (Fig. 7B, right). Levels of insulin regulation of PKB/Akt and other signaling components of the pathway, such as phosphorylation of extracellular signal-regulated kinase (ERK) and S6K, remained similar in both liver and SM extracts from both the MβKO and the FL/FLβ control mice (Fig. 7C). Interestingly, however, we observed a significantly elevated basal phosphorylation of GSK-3α in the SM of MβKO mice. Furthermore, kinase assays performed on SM extracts from the MβKO mice revealed a larger-than-expected reduction in total GSK-3 activity compared to the level for FL/FLβ control animals (Fig. 7D). GSK-3 activity was reduced by approximately 70% (to 28.6% ± 8% of FL/FLβ levels), and this was not accompanied by changes in GSK-3α expression (Fig. 7A). Together, these findings suggest that GSK-3β activity plays a greater role than GSK-3α in regulating GS in SM. Kinase assays performed on SM and liver extracts from GSK-3α KO mice revealed that total GSK-3 activity was reduced by approximately 40 to 50% in each tissue for liver (to 58.0% ± 8% of WT levels) and for SM (to 62% ± 7% of WT levels) (see Fig. S3 in the supplemental material).

In addition to the lower total GSK-3 activity and more-active GS, we also observed elevated glycogen storage within the SM of the MβKO mice (Fig. 8A). To assess whether changes in components of the glucose transport machinery accounted for the increase in glycogen storage observed in the SM of the MβKO mice, the relative expression levels of glucose transporters that promote the uptake of glucose into SM were quantified. No significant changes were observed in the total cell membrane expression of the GLUT1 or the insulin-regulated GLUT4 glucose transporters in SM homogenates from the MβKO mice (Fig. 8B). We next determined the rates of glucose transport in isolated EDL and soleus muscles. While there was a trend for the rate of glucose transport to be higher in the insulin-stimulated EDL muscles of the MβKO mice than in those of the FL/FLβ control mice, this did not reach statistical significance. Using [^{3}H]2DG as a tracer, we performed in vivo glucose uptake measurements during an i.p. GTT and determined that the uptakes of 2DG in muscle tissue were similar in both MβKO and FL/FLβ control mice (Fig. 8D). We next examined whether alteration in the glycogen degradation process could account for the differences observed in the MβKO mice. No significant changes were observed in the expression, phosphorylation (Fig. 8E, left), or activity (right) levels of glycogen phosphorylase, the enzyme that catalyzes the rate-limiting step of glycogenolysis.

DISCUSSION

Here, we describe the generation and characterization of tissue-specific genetic deletions of GSK-3β and the impacts of inactivation of this enzyme in two tissues (SM and liver) on glucose metabolism and insulin sensitivity. A central finding of this conditional KO mouse analysis is that deletion of GSK-3β from SM results in improved glucose tolerance and enhanced insulin sensitivity. In contrast, specific inactivation in liver had no effect on glucose metabolism or insulin responsiveness. The effects in the SM KO of GSK-3β were associated with potentiation of insulin-induced dephosphorylation and activation of GS and increased glycogen deposition in SM. These data are consistent with previous studies demonstrating that inhibitors of GSK-3 (that inactivate both GSK-3α and GSK-3β) can stimulate GS activity and glycogen deposition within SM (10, 22, 29, 31). Our genetic data show that GSK-3β is the major regulator of GS in SM. Indeed, transgenic overexpression of GSKβ in the SM of mice leads to glucose intolerance, together with a reduction in both GS activation and muscle glycogen content (36). Furthermore, McManus et al. demonstrated that insulin regulation of GS was completely abolished in the SM of homozygous "knock-in" mice expressing a point mutation in an insulin-insensitive phosphorylation site (serine 9) of GSK-3β, whereas in the equivalent GSK-3α knock-in mutant mice (serine 21), GS activity was unaltered (30). The tissue-specific effect observed for GSK-3β over GSK-3α on GS regulation in murine SM could be explained in part by the higher relative levels of expression of the GSK-3β isoform in muscle. Indeed, for human SM it has been reported that GSK-3β is more abundant than GSK-3α, implicating GSK-3β as the major regulator of glucose metabolism in human SM (30).

In our studies, we find that GSK-3α and GSK-3β protein levels in murine SM are essentially equivalent (44.9% ± 0.9% for GSK-3α versus 54.6% ± 1.3% for GSK-3β). That said, there is a greater-than-expected reduction (~75%) in total GSK-3 activity in SM extracts from the MβKO mice, compared with a 50 to 55% reduction in total GSK-3 activity observed when GSK-3β is deleted within the liver or in tissues that lack GSK-3α (see Fig. S3 in the supplemental material). Further-

incubation with 20 nM insulin. At the times indicated, cells were lysed and the lysates subjected to SDS-polyacrylamide gel electrophoresis and immunoblotted with the indicated antibodies. A representative blot is shown (left), with quantification of results from four independent experiments displayed (right). NS, not significant. (C) GSK-3 kinase assays. Liver tissues were extracted from 8-week-old male FL/FLβ control and LβKO mice and partially purified through a CM-Sepharose column as described in Materials and Methods. GSK-3 kinase activities were determined using a quantitative peptide phosphorylation assay and are expressed relative to that for the FL/FLβ control (which is set at 100%). Values are the means ± SEMs of results for five different livers, with each assayed in triplicate. (D) GS activity. Liver tissues were extracted from 8-week-old male FL/FLβ control and LβKO mice and homogenized, and GS activity was measured in the presence of 0.1 mM (low) or 10 mM (high) G6P as described in Materials and Methods. Values are the means ± SEMs of results from four different livers, with each assayed in duplicate. **, $P < 0.01$ (for comparison to fasted mice for each genotype); NS, not significant (for comparison to fasted FL/FLβ mice).

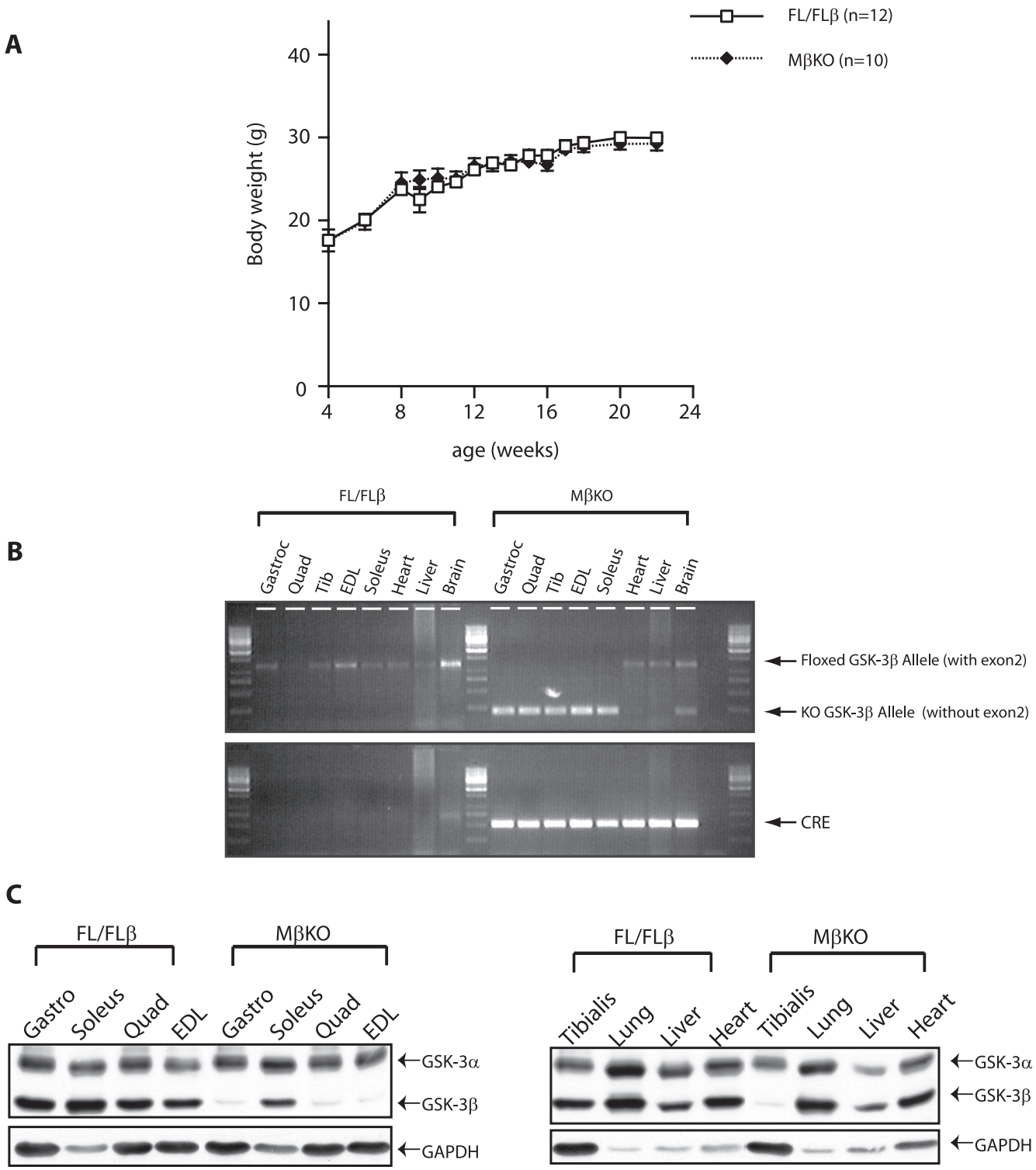

FIG. 5. Generation of SM-specific GSK-3β KO (MβKO) mice. (A) Weight analysis. Male FL/FLβ control and GSK-3β FL/FL mlc1*f* Cre^{+} (termed MβKO) mice were weighed every week between the ages of 4 and 24 weeks. Each point represents the mean ± SEM, with *n* indicating the number analyzed in each group. No statistical differences in mean weight were observed between the groups by Student's *t* test. (B) PCR analysis. Genomic DNA was isolated from the tissues stated and analyzed by PCR for Cre-mediated excision of GSK-3β. PCR for GSK-3β (top) demonstrates that exon 2 of the GSK-3β FL allele was excised in all SM types of the MβKO mice but not the control FL/FLβ. The bottom panel indicates genomic detection of the Cre transgene. Gastroc, gastrocnemius. (C) Western blot analysis. Tissue extracts were prepared from 8-week-old male mice of the genotypes indicated and immunoblotted with an antibody that recognizes GSK-3α and GSK-3β. The loading of the lanes was assessed using an anti-GAPDH antibody, and the blots are representative of three independent experiments. Gastro, gastrocnemius.

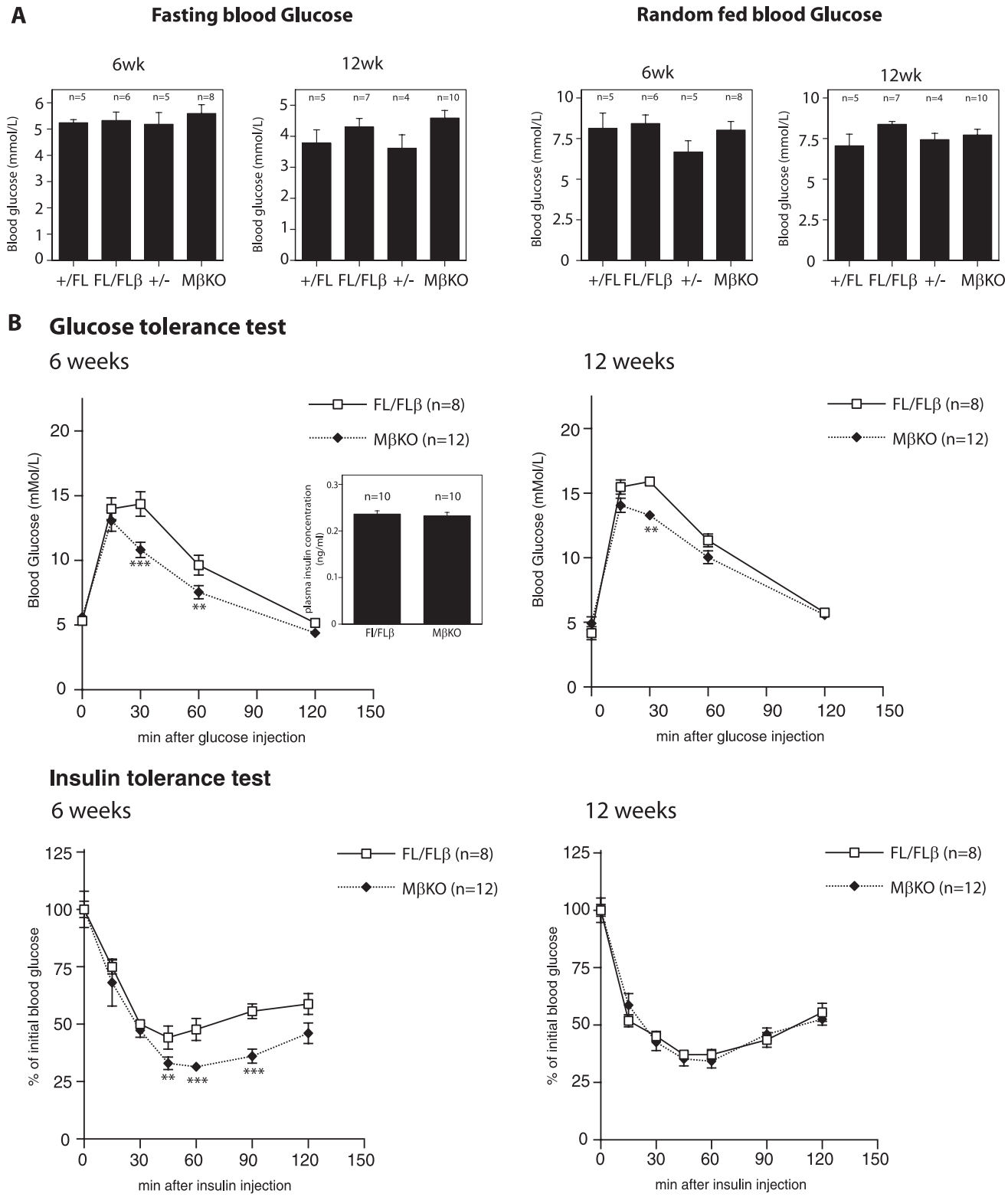

FIG. 6. MβKO mice display improved glucose homeostasis and insulin sensitivity. (A) Blood glucose profile. Six- or 12-week-old male FL/FLβ control and MβKO mice were either fasted overnight for 16 h (fasted) or fed ad libitum (random fed), and blood glucose levels were measured. The data are presented as means ± SEMs, with the number (*n*) of mice in each group indicated. (B) Glucose metabolism profile. GTT and ITT were performed on 6-week- or 12-week-old male FL/FLβ control and MβKO mice as described in Materials and Methods. The inset depicts the plasma insulin concentrations in the FL/FLβ and MβKO mice following a 15-min i.p. injection of glucose. Values are means ± SEMs, with *n* indicating the number of mice in each group. Asterisks signify statistically significant changes compared to levels for the FL/FLβ control mice. *, $P < 0.05$; **, $P < 0.01$; ***, $P < 0.001$.

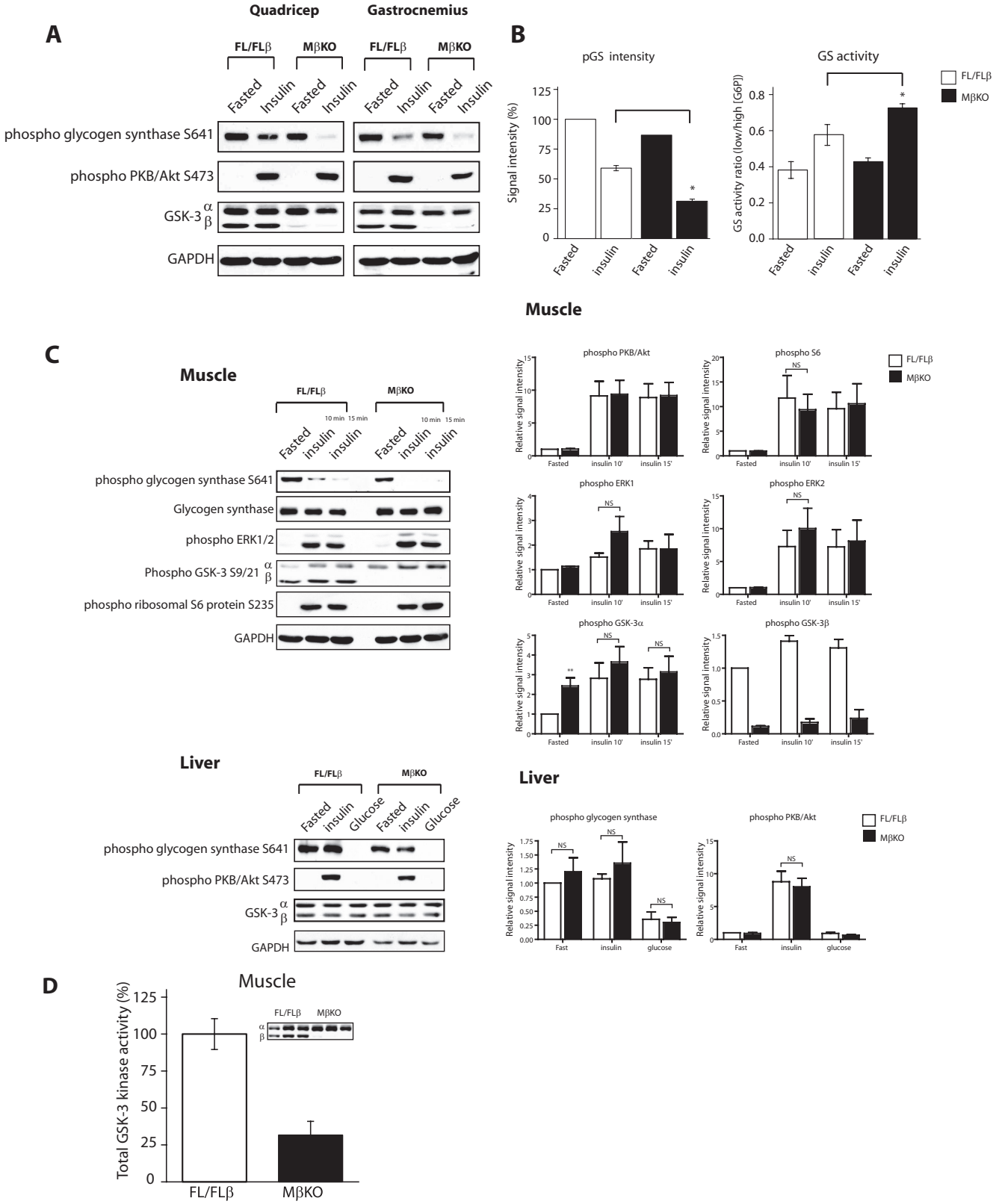

FIG. 7. Analysis of insulin signaling in MβKO mice. (A and C) Insulin signaling in muscle (A and C, top) and liver (C, bottom). Six-week-old male FL/FLβ control and MβKO mice were fasted overnight and injected i.p. with 100 mU/g insulin or with 1 mg/g glucose for 20 min or for the times indicated. Following treatment, different SM types (top panels) and liver tissue (bottom left) were extracted, lysed as described in Materials and Methods, and immunoblotted with the indicated antibodies. A representative blot is shown (left), with the quantifications of results from at least four independent experiments displayed (right). *, $P < 0.05$; NS, not significant. (B) GS regulation. (Left) Signal intensities of the

more, the insulin-induced changes in GSK-3 activity were similar in muscle extracts from FL/FLβ control and MβKO mice (see Fig. S4 in the supplemental material). In this study, we also find that as the MβKO mice age, their capacity to maintain improved glucose tolerance and insulin sensitivity diminishes. While glucose tolerance becomes less pronounced by age (6 months) (see Fig. S4 in the supplemental material), insulin sensitivity and glycogen accretion are lost by 12 weeks (insulin tolerance is lost at 6 months) (see Fig. S4 in the supplemental material). We investigated the possibility that there was an age-dependent compensatory increase in GSK-3α that overcame the sensitization effects in the MβKO mice. However, while there was increased expression of GSK-3α in aged mice, levels of this were comparable in both MβKO mice and FL/FLβ controls (see Fig. S5 in the supplemental material). Thus, we speculate that the apparent loss in glucose and insulin tolerance in the MβKO mice may be explained by the commonly observed decrease in insulin responsiveness that occurs with aging (12). Indeed, young animals as well as mildly (but not severely) diabetic animal models show a greater responsiveness in lowering blood glucose when treated with GSK-3 inhibitors (47).

Previous studies have demonstrated that application of GSK-3 inhibitors to isolated SM enhances insulin signaling (14, 22, 32, 40). In addition to its effects on GS regulation, these GSK-3 inhibitors also potentiated insulin-stimulated phosphorylation of PKB/Akt. This observation was explained by previous findings demonstrating that GSK-3 can phosphorylate and negatively regulate insulin receptor substrate 1 (IRS-1), impairing downstream insulin signaling. While we do not see significant differences in PKB or S6K phosphorylation in the MβKO mice, there is a significant increase in basal serine phosphorylation of GSK-3α, in addition to enhanced GS regulation. The mechanism by which this occurs may not be due to upregulation of IRS1/PKB but may be explained by the fact that, in addition to PKB, several other kinases (PKC, PKA, p90rsk, and S6K) can phosphorylate GSK-3 (18, 19, 43, 52). It is possible that increases in the activities of these kinases may mediate GSK-3 phosphorylation. Indeed, there is a trend, though not statistically significant, for upregulation of ERK in the MβKO mice (Fig. 7C). GSK-3 is a known negative regulator of ERK/Jun N-terminal protein kinase signaling (1, 26, 48), and there is evidence to suggest that GSK-3 regulates the activity of a protein phosphatase, which in turn regulates GSK-3 itself (51).

Net glycogen content is coordinately and simultaneously regulated by both synthesis and breakdown. We addressed whether changes in these processes accounted for the elevated glycogen deposition in the MβKO animals. From this study, it is clear that glycogen synthesis is, in part, mediating glycogen accretion in the MβKO mice. Insulin-stimulated GS activity is consistently elevated in the SM of MβKO mice. While this form of GS regulation is most likely the significant contributor toward glycogen status in fed mice, the mechanism by which glycogen is elevated in fasting mice is unclear (since GS activity remained similar to that for FL/FLβ). We tested whether the glucose transport machinery was altered in the MβKO mice. The expression of the insulin-sensitive GLUT4 transporter remained unchanged. In addition, there were no significant differences in the rates of basal and insulin-stimulated glucose transport in isolated muscle tissues or in vivo. Furthermore, there appeared to be no alteration in the glycogen breakdown pathway as assessed by glycogen phosphorylase regulation. Thus, at present, the mechanism underlying the elevated glycogen in fasted MβKO mice is unresolved. One explanation for the higher glycogen levels is that the MβKO mice display lower muscle activity. Anecdotal observation of these mice has not revealed an obvious difference in movement compared to levels for WT littermates, although more-subtle differences in activity would require more-extensive study to reveal. It is also possible that the MβKO mice have adapted to utilizing alternative fuels, such as free fatty acids, thereby "shunting" glucose toward glycogen. However, we observed no differences in adiposity (as determined by fat pad weights, adiponectin, and triglyceride levels) (see Fig. S6 in the supplemental material) in our studies that would account for improved glycogen storage, glucose tolerance, and insulin sensitivity. It will be of interest to examine whether any changes occur in the insulin signaling profile or glucose metabolism in MβKO mice that are subjected to a high-fat diet to promote insulin resistance or that are bred onto a genetically obese background.

Deletion of hepatic GSK-3β resulted in a minimal phenotype with regard to glucose regulation and insulin signaling, although we cannot exclude the possibility that certain metabolic phenotypes may manifest themselves only under conditions of insulin resistance (high-fat diet or ob/ob background). Based on the finding that the global GSK-3β KO mice die in embryogenesis from massive liver apoptosis, our original hypothesis was that the LβKO mice would present a similar phenotype (23). However, LβKO mice are viable and show no abnormalities within the liver or whole body. As the albumin gene (and hence Cre) is not efficiently expressed during embryogenesis (38), we were unable to determine whether embryonic deletion of hepatic GSK-3β would recapitulate the lethality of the global GSK-3β KO. However, hepatocytes isolated from 8- to 12-week-old LβKO mice (when Cre is maxi-

insulin-stimulated dephosphorylation of GS from muscle (gastrocnemius) tissues of the FL/FLβ control and MβKO mice were quantified, and the data are presented as a bar graph showing signal intensities as percentages of the WT level (100%). Values are the means ± SEMs from at least four independent experiments. *, $P < 0.05$ (FL/Flβ versus MβKO, insulin treated). (Right) Muscle tissues were extracted from 6-week-old male FL/FLβ control and MβKO mice and homogenized, and GS activity was measured in the presence of 0.1 mM (low) or 10 mM (high) G6P as described in Materials and Methods. Values are the means ± SEMs of results from six different muscle samples, with each assayed in duplicate. *, $P < 0.05$ (FL/Flβ versus MβKO, insulin treated). (D) GSK-3 kinase assays. Muscle (gastrocnemius) tissue was extracted from 6-week-old male FL/FLβ control and MβKO mice and partially purified with CM-Sepharose chromatography as described in Materials and Methods. GSK-3 kinase activity was determined using a quantitative peptide phosphorylation assay. The inset shows an immunoblot of GSK-3 that was used in the kinase assay reaction. GSK-3 kinase activities are expressed relative to that for the FL/FLβ control (which is set at 100%) and are the means ± SEMs of results from five different muscle samples, with each assayed in triplicate.

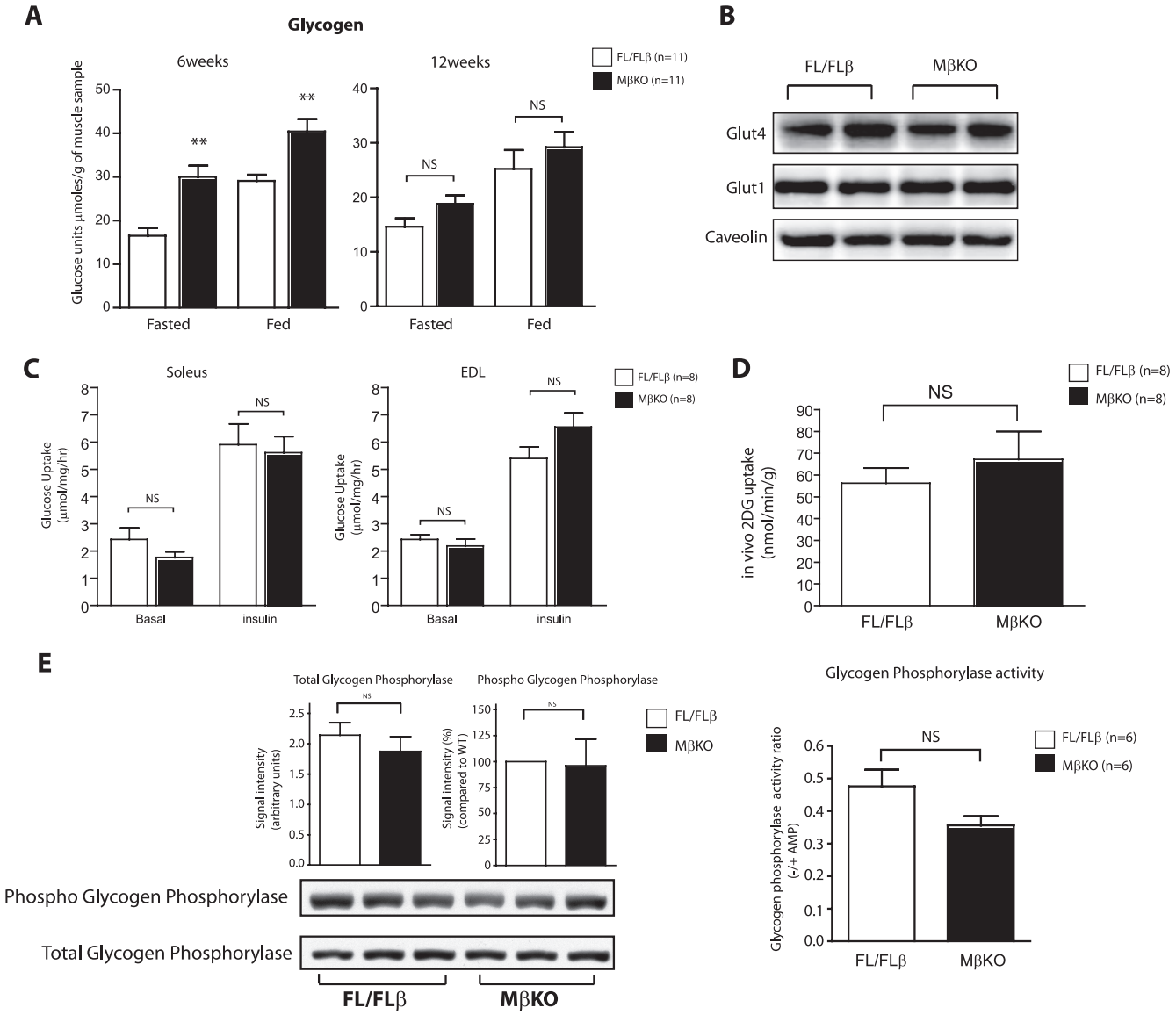

FIG. 8. Analysis of glycogen deposition and glucose transport in MβKO mice. (A) Glycogen content in muscle. Muscle tissue (gastrocnemius) was extracted from fasted (overnight, 16 h) or fed (ad libitum) 6- or 12-week-old male FL/FLβ control and MβKO mice, and glycogen content was determined by acid hydrolysis and expressed as μmol of glucose units per gram of muscle tissue. The data are presented as means ± SEMs, with each muscle sample assayed in triplicate, and *n* indicates the number of mice in each group. *, $P < 0.05$; NS, not significant. (B) GLUT4 expression analysis. Muscle tissue (gastrocnemius) was extracted from 6-week-old male FL/FLβ control and MβKO mice and total cell membrane isolated as described in Materials and Methods and immunoblotted with the indicated antibodies. Equal loading of the lanes was assessed using an anticaveolin antibody, and the blots shown are representative of at least four independent experiments. (C) In vitro glucose transport measurement. Intact soleus and EDL muscle fibers were isolated from deeply anesthetized FL/FLβ control and MβKO mice and were incubated with or without 2 mU of insulin per ml for 30 min. 2-Deoxy-D-glucose uptake was measured over a 20-min period as described in Materials and Methods. The data are presented as means ± SEMs, with the number (*n*) of mice in each group indicated. NS, not significant. (D) In vivo glucose uptake. Six-week-old male FL/FLβ control and MβKO mice were fasted overnight and injected i.p. with a mixture of unlabeled dextrose and [^{3}H]2DG, and the accumulation of the 2DG in muscle tissue (gastrocnemius) was determined as described in Materials and Methods. Data are presented as means ± SEMs, with the number (*n*) of mice in each group indicated. (E) Glycogen phosphorylase regulation. (Left) Muscle tissue (gastrocnemius) was extracted from 6-week-old male FL/FLβ control and MβKO mice and immunoblotted with the indicated antibodies. A representative blot is shown (below), with quantification of results from three independent experiments displayed as a bar graph (above). Total glycogen phosphorylase expression was normalized to GAPDH levels and expressed as signal intensities, while the signal intensities from the phosphorylated form of the protein are expressed relative to the WT level (100%). (Right) Muscle tissues were extracted from male FL/FLβ control and MβKO mice and homogenized, and glycogen phosphorylase activity was measured in the absence or presence of AMP as described in Materials and Methods.

mally expressed) displayed increased sensitivity to tumor necrosis factor alpha-induced apoptosis (data not shown), consistent with previous data that have shown that GSK-3β KO mouse embryonic fibroblasts have elevated susceptibility to tumor necrosis factor alpha-mediated cell death and defects in NF-κB signaling (23, 42, 44).

The tissue-selective effects of GSK-3 isoform inactivation indicate the existence of isoform- and tissue-specific roles for

GSK-3 in the regulation of glucose metabolism. Indeed, Tanabe et al. demonstrate that mice heterozygous for GSK-3β preserve β-cell integrity and reduce the onset of diabetes in two genetic models of this disease (45). Furthermore, using the GSK-3β-floxed lines described here, Tanabe et al. generated islet-specific GSK-3β KO mice. These animals show a reduction in the age-dependent hyperglycemia normally observed in IRS-2 KO mice, suggesting that islet GSK-3β is required for the chronic elevation of blood glucose in this model (45). Furthermore, we have recently generated mice that lack GSK-3α expression in all tissues. Unlike their global GSK-3β KO counterparts, GSK-3α-null mice are viable but display enhanced hepatic insulin sensitivity and glucose homeostasis (28). However, the SM of these animals exhibited normal insulin signaling, GS regulation, and glycogen deposition.

Therefore, the findings presented in this study, along with the phenotypes associated with the GSK-3α and GSK-3β KO mice, demonstrate that the two mammalian isoforms of GSK-3 each have distinct as well as overlapping biological roles. On the one hand, GSK-3α and GSK-3β appear to be equally important in regulating Wnt/β-catenin signaling (13). However, GSK-3α has a more critical role than GSK-3β in regulating hepatic glucose metabolism and insulin sensitivity (28), and GSK-3β is the predominant regulator of GS in SM. We speculate that the functional dominance of either GSK-3α or GSK-3β within individual tissues is determined by selective association with targets through their noncatalytic domains, possibly via adaptor or scaffolding proteins. Our studies also suggest that intermediate inhibition of both forms of GSK-3 is necessary for insulin resensitization effects in muscle and liver tissues in T2DM.

ACKNOWLEDGMENTS

We thank T. Hansotia (SLRI) and G. Wiggin (SLRI) for critical review of the manuscript and discussion and M. Woo, A. Klip, A. Tung, and K. Sakamoto for valuable technical advice and assistance. We thank J. Guinovart (University of Barcelona), P. T. Cohen (University of Dundee), and S. Burden (Skirball Institute, NY) for reagents.

Funding for this work was provided by the Canadian Institutes of Health Research (J.R.W. [MOP 74711], S.P., and B.W.D.), the Canadian Diabetes Association (J.R.W.), and the Banting and Best Diabetes Centre (J.R.W., S.P., and K.M.).

REFERENCES

1. **Abell, A. N., D. A. Granger, and G. L. Johnson.** 2007. MEKK4 stimulation of p38 and JNK activity is negatively regulated by GSK3beta. J. Biol. Chem. **282:**30476–30484.
2. **Bajaj, M., and R. A. Defronzo.** 2003. Metabolic and molecular basis of insulin resistance. J. Nucl. Cardiol. **10:**311–323.
3. **Bollen, M., S. Keppens, and W. Stalmans.** 1998. Specific features of glycogen metabolism in the liver. Biochem. J. **336:**19–31.
4. **Bondar, R. J., and D. C. Mead.** 1974. Evaluation of glucose-6-phosphate dehydrogenase from Leuconostoc mesenteroides in the hexokinase method for determining glucose in serum. Clin. Chem. **20:**586–590.
5. **Bothe, G. W., J. A. Haspel, C. L. Smith, H. H. Wiener, and S. J. Burden.** 2000. Selective expression of Cre recombinase in skeletal muscle fibers. Genesis **26:**165–166.
6. **Bouche, C., S. Serdy, C. R. Kahn, and A. B. Goldfine.** 2004. The cellular fate of glucose and its relevance in type 2 diabetes. Endocr. Rev. **25:**807–830.
7. **Bouskila, M., M. F. Hirshman, J. Jensen, L. J. Goodyear, and K. Sakamoto.** 2008. Insulin promotes glycogen synthesis in the absence of GSK3 phosphorylation in skeletal muscle. Am. J. Physiol. Endocrinol. Metab. **294:**E28–E35.
8. **Cheng, K., S. Creacy, and J. Larner.** 1983. 'Insulin-like' effects of lithium ion on isolated rat adipocytes. II. Specific activation of glycogen synthase. Mol. Cell. Biochem. **56:**183–189.
9. **Cline, G. W., K. Johnson, W. Regittnig, P. Perret, E. Tozzo, L. Xiao, C. Damico, and G. I. Shulman.** 2002. Effects of a novel glycogen synthase kinase-3 inhibitor on insulin-stimulated glucose metabolism in Zucker diabetic fatty (fa/fa) rats. Diabetes **51:**2903–2910.
10. **Coghlan, M. P., A. A. Culbert, D. A. Cross, S. L. Corcoran, J. W. Yates, N. J. Pearce, O. L. Rausch, G. J. Murphy, P. S. Carter, L. Roxbee Cox, D. Mills, M. J. Brown, D. Haigh, R. W. Ward, D. G. Smith, K. J. Murray, A. D. Reith, and J. C. Holder.** 2000. Selective small molecule inhibitors of glycogen synthase kinase-3 modulate glycogen metabolism and gene transcription. Chem. Biol. **7:**793–803.
11. **Cross, D. A., D. R. Alessi, P. Cohen, M. Andjelkovich, and B. A. Hemmings.** 1995. Inhibition of glycogen synthase kinase-3 by insulin mediated by protein kinase B. Nature **378:**785–789.
12. **DeFronzo, R. A.** 1981. Glucose intolerance and aging. Diabetes Care **4:**493–501.
13. **Doble, B. W., S. Patel, G. A. Wood, L. K. Kockeritz, and J. R. Woodgett.** 2007. Functional redundancy of GSK-3alpha and GSK-3beta in Wnt/beta-catenin signaling shown by using an allelic series of embryonic stem cell lines. Dev. Cell **12:**957–971.
14. **Dokken, B. B., J. A. Sloniger, and E. J. Henriksen.** 2005. Acute selective glycogen synthase kinase-3 inhibition enhances insulin signaling in pre-diabetic insulin-resistant rat skeletal muscle. Am. J. Physiol. Endocrinol. Metab. **288:**E1188–E1194.
15. **Eldar-Finkelman, H., G. M. Argast, O. Foord, E. H. Fischer, and E. G. Krebs.** 1996. Expression and characterization of glycogen synthase kinase-3 mutants and their effect on glycogen synthase activity in intact cells. Proc. Natl. Acad. Sci. USA **93:**10228–10233.
16. **Eldar-Finkelman, H., S. A. Schreyer, M. M. Shinohara, R. C. LeBoeuf, and E. G. Krebs.** 1999. Increased glycogen synthase kinase-3 activity in diabetes- and obesity-prone C57BL/6J mice. Diabetes **48:**1662–1666.
17. **Embi, N., D. B. Rylatt, and P. Cohen.** 1980. Glycogen synthase kinase-3 from rabbit skeletal muscle. Separation from cyclic-AMP-dependent protein kinase and phosphorylase kinase. Eur. J. Biochem. **107:**519–527.
18. **Fang, X., S. Yu, J. L. Tanyi, Y. Lu, J. R. Woodgett, and G. B. Mills.** 2002. Convergence of multiple signaling cascades at glycogen synthase kinase 3: Edg receptor-mediated phosphorylation and inactivation by lysophosphatidic acid through a protein kinase C-dependent intracellular pathway. Mol. Cell. Biol. **22:**2099–2110.
19. **Fang, X., S. X. Yu, Y. Lu, R. C. Bast, Jr., J. R. Woodgett, and G. B. Mills.** 2000. Phosphorylation and inactivation of glycogen synthase kinase 3 by protein kinase A. Proc. Natl. Acad. Sci. USA **97:**11960–11965.
20. **Frame, S., and D. Zheleva.** 2006. Targeting glycogen synthase kinase-3 in insulin signalling. Expert Opin. Ther. Targets **10:**429–444.
21. **Hansen, L., K. C. Arden, S. B. Rasmussen, C. S. Viars, H. Vestergaard, T. Hansen, A. M. Moller, J. R. Woodgett, and O. Pedersen.** 1997. Chromosomal mapping and mutational analysis of the coding region of the glycogen synthase kinase-3alpha and beta isoforms in patients with NIDDM. Diabetologia **40:**940–946.
22. **Henriksen, E. J., T. R. Kinnick, M. K. Teachey, M. P. O'Keefe, D. Ring, K. W. Johnson, and S. D. Harrison.** 2003. Modulation of muscle insulin resistance by selective inhibition of GSK-3 in Zucker diabetic fatty rats. Am. J. Physiol. Endocrinol. Metab. **284:**E892–E900.
23. **Hoeflich, K. P., J. Luo, E. A. Rubie, M. S. Tsao, O. Jin, and J. R. Woodgett.** 2000. Requirement for glycogen synthase kinase-3beta in cell survival and NF-kappaB activation. Nature **406:**86–90.
24. **Kaidanovich-Beilin, O., and H. Eldar-Finkelman.** 2006. Long-term treatment with novel glycogen synthase kinase-3 inhibitor improves glucose homeostasis in ob/ob mice: molecular characterization in liver and muscle. J. Pharmacol. Exp. Ther. **316:**17–24.
25. **Lawrence, J. C., Jr., and P. J. Roach.** 1997. New insights into the role and mechanism of glycogen synthase activation by insulin. Diabetes **46:**541–547.
26. **Liu, S., S. Yu, Y. Hasegawa, R. Lapushin, H. J. Xu, J. R. Woodgett, G. B. Mills, and X. Fang.** 2004. Glycogen synthase kinase 3beta is a negative regulator of growth factor-induced activation of the c-Jun N-terminal kinase. J. Biol. Chem. **279:**51075–51081.
27. **Lochhead, P. A., M. Coghlan, S. Q. Rice, and C. Sutherland.** 2001. Inhibition of GSK-3 selectively reduces glucose-6-phosphatase and phosphatase and phosphoenolypyruvate carboxykinase gene expression. Diabetes **50:**937–946.
28. **MacAulay, K., B. W. Doble, S. Patel, T. Hansotia, E. M. Sinclair, D. J. Drucker, A. Nagy, and J. R. Woodgett.** 2007. Glycogen synthase kinase 3alpha-specific regulation of murine hepatic glycogen metabolism. Cell Metab. **6:**329–337.
29. **MacAulay, K., E. Hajduch, A. S. Blair, M. P. Coghlan, S. A. Smith, and H. S. Hundal.** 2003. Use of lithium and SB-415286 to explore the role of glycogen synthase kinase-3 in the regulation of glucose transport and glycogen synthase. Eur. J. Biochem. **270:**3829–3838.
30. **McManus, E. J., K. Sakamoto, L. J. Armit, L. Ronaldson, N. Shpiro, R. Marquez, and D. R. Alessi.** 2005. Role that phosphorylation of GSK3 plays in insulin and Wnt signalling defined by knockin analysis. EMBO J. **24:**1571–1583.
31. **Nikoulina, S. E., T. P. Ciaraldi, L. Carter, S. Mudaliar, K. S. Park, and R. R. Henry.** 2001. Impaired muscle glycogen synthase in type 2 diabetes is asso-

ciated with diminished phosphatidylinositol 3-kinase activation. J. Clin. Endocrinol. Metab. **86:**4307–4314.
32. **Nikoulina, S. E., T. P. Ciaraldi, S. Mudaliar, L. Carter, K. Johnson, and R. R. Henry.** 2002. Inhibition of glycogen synthase kinase 3 improves insulin action and glucose metabolism in human skeletal muscle. Diabetes **51:**2190–2198.
33. **Nikoulina, S. E., T. P. Ciaraldi, S. Mudaliar, P. Mohideen, L. Carter, and R. R. Henry.** 2000. Potential role of glycogen synthase kinase-3 in skeletal muscle insulin resistance of type 2 diabetes. Diabetes **49:**263–271.
34. **Orena, S. J., A. J. Torchia, and R. S. Garofalo.** 2000. Inhibition of glycogen-synthase kinase 3 stimulates glycogen synthase and glucose transport by distinct mechanisms in 3T3-L1 adipocytes. J. Biol. Chem. **275:**15765–15772.
35. **Parker, P. J., F. B. Caudwell, and P. Cohen.** 1983. Glycogen synthase from rabbit skeletal muscle; effect of insulin on the state of phosphorylation of the seven phosphoserine residues in vivo. Eur. J. Biochem. **130:**227–234.
36. **Pearce, N. J., J. R. Arch, J. C. Clapham, M. P. Coghlan, S. L. Corcoran, C. A. Lister, A. Llano, G. B. Moore, G. J. Murphy, S. A. Smith, C. M. Taylor, J. W. Yates, A. D. Morrison, A. J. Harper, L. Roxbee-Cox, A. Abuin, E. Wargent, and J. C. Holder.** 2004. Development of glucose intolerance in male transgenic mice overexpressing human glycogen synthase kinase-3beta on a muscle-specific promoter. Metabolism **53:**1322–1330.
37. **Petersen, K. F., and G. I. Shulman.** 2006. Etiology of insulin resistance. Am. J. Med. **119:**S10–S16.
38. **Postic, C., and M. A. Magnuson.** 2000. DNA excision in liver by an albumin-Cre transgene occurs progressively with age. Genesis **26:**149–150.
39. **Postic, C., M. Shiota, K. D. Niswender, T. L. Jetton, Y. Chen, J. M. Moates, K. D. Shelton, J. Lindner, A. D. Cherrington, and M. A. Magnuson.** 1999. Dual roles for glucokinase in glucose homeostasis as determined by liver and pancreatic beta cell-specific gene knock-outs using Cre recombinase. J. Biol. Chem. **274:**305–315.
40. **Ring, D. B., K. W. Johnson, E. J. Henriksen, J. M. Nuss, D. Goff, T. R. Kinnick, S. T. Ma, J. W. Reeder, I. Samuels, T. Slabiak, A. S. Wagman, M. E. Hammond, and S. D. Harrison.** 2003. Selective glycogen synthase kinase 3 inhibitors potentiate insulin activation of glucose transport and utilization in vitro and in vivo. Diabetes **52:**588–595.
41. **Shulman, G. I.** 2004. Unraveling the cellular mechanism of insulin resistance in humans: new insights from magnetic resonance spectroscopy. Physiology (Bethesda) **19:**183–190.
42. **Steinbrecher, K. A., W. Wilson III, P. C. Cogswell, and A. S. Baldwin.** 2005. Glycogen synthase kinase 3β functions to specify gene-specific, NF-κB-dependent transcription. Mol. Cell. Biol. **25:**8444–8455.
43. **Sutherland, C., I. A. Leighton, and P. Cohen.** 1993. Inactivation of glycogen synthase kinase-3 beta by phosphorylation: new kinase connections in insulin and growth-factor signalling. Biochem. J. **296:**15–19.
44. **Takada, Y., X. Fang, M. S. Jamaluddin, D. D. Boyd, and B. B. Aggarwal.** 2004. Genetic deletion of glycogen synthase kinase-3beta abrogates activation of IkappaBalpha kinase, JNK, Akt, and p44/p42 MAPK but potentiates apoptosis induced by tumor necrosis factor. J. Biol. Chem. **279:**39541–39554.
45. **Tanabe, K., Z. Liu, S. Patel, B. W. Doble, L. Li, C. Cras-Meneur, S. C. Martinez, C. M. Welling, M. F. White, E. Bernal-Mizrachi, J. R. Woodgett, and M. A. Permutt.** 2008. Genetic deficiency of glycogen synthase kinase-3beta corrects diabetes in mouse models of insulin resistance. PLoS Biol. **6:**e37.
46. **Thomas, J. A., K. K. Schlender, and J. Larner.** 1968. A rapid filter paper assay for UDPglucose-glycogen glucosyltransferase, including an improved biosynthesis of UDP-14C-glucose. Anal. Biochem. **25:**486–499.
47. **Wagman, A. S., K. W. Johnson, and D. E. Bussiere.** 2004. Discovery and development of GSK3 inhibitors for the treatment of type 2 diabetes. Curr. Pharm. Des. **10:**1105–1137.
48. **Wang, Q., Y. Zhou, X. Wang, and B. M. Evers.** 2006. Glycogen synthase kinase-3 is a negative regulator of extracellular signal-regulated kinase. Oncogene **25:**43–50.
49. **Wijesekara, N., D. Konrad, M. Eweida, C. Jefferies, N. Liadis, A. Giacca, M. Crackower, A. Suzuki, T. W. Mak, C. R. Kahn, A. Klip, and M. Woo.** 2005. Muscle-specific Pten deletion protects against insulin resistance and diabetes. Mol. Cell. Biol. **25:**1135–1145.
50. **Woodgett, J. R.** 1990. Molecular cloning and expression of glycogen synthase kinase-3/factor A. EMBO J. **9:**2431–2438.
51. **Zhang, F., C. J. Phiel, L. Spece, N. Gurvich, and P. S. Klein.** 2003. Inhibitory phosphorylation of glycogen synthase kinase-3 (GSK-3) in response to lithium. Evidence for autoregulation of GSK-3. J. Biol. Chem. **278:**33067–33077.
52. **Zhang, H. H., A. I. Lipovsky, C. C. Dibble, M. Sahin, and B. D. Manning.** 2006. S6K1 regulates GSK3 under conditions of mTOR-dependent feedback inhibition of Akt. Mol. Cell **24:**185–197.
53. **Zisman, A., O. D. Peroni, E. D. Abel, M. D. Michael, F. Mauvais-Jarvis, B. B. Lowell, J. F. Wojtaszewski, M. F. Hirshman, A. Virkamaki, L. J. Goodyear, C. R. Kahn, and B. B. Kahn.** 2000. Targeted disruption of the glucose transporter 4 selectively in muscle causes insulin resistance and glucose intolerance. Nat. Med. **6:**924–928.